

Pulsed bismuth fibre laser with the intracavity-compensated group velocity dispersion

A.A. Krylov, P.G. Kryukov, E.M. Dianov, O.G. Okhotnikov, M. Guina

Abstract. Passive mode locking is achieved in a bismuth-doped fibre laser with the help of a SESAM saturable absorber optimised for operation in the spectra range from 1100 to 1200 nm. Pumping was performed by a 2-W cw ytterbium fibre laser at 1075 nm. The oscillation of the laser with an intracavity group-velocity-dispersion compensator based on a pair of diffraction gratings is studied. Laser pulses with the minimum duration of ~ 5 ps are generated.

Keywords: bismuth fibre laser, mode locking, SESAM, group-velocity-dispersion compensation.

1. Introduction

Interest in the study of bismuth-doped optical fibres is related to attempts to expand the spectral range of fibre lasers and amplifiers to the region of the second transparency window (~ 1.3 μm) of silica fibres. At present the cw emission of bismuth fibre lasers was obtained between 1140 and 1215 nm [1–4] upon pumping by an ytterbium fibre laser and between 1.3 and 1.5 μm [5] upon pumping by either a Raman fibre laser at 1230 nm or a bismuth fibre laser at 1205 nm. The lasing efficiency at a wavelength of 1160 nm achieves 50% at 77 K and 30% at 300 K [6], which, aside from the rest, suggests that it is possible to develop a high-power narrowband laser emitting in the yellow range, which is required for the creation of an ‘artificial star’ used in astronomy to correct the adaptive optics of large telescopes [7]. The spectral range between 1.3 and 1.5 μm is of interest for telecommunications [8].

A broad luminescence spectrum of active bismuth centres in fibres gives grounds to assume that it is possible to generate ultrashort subpicosecond pulses in the mode-locking regime. However, such fibres have an important disadvantage of a low concentration of bismuth centres, which requires the use of very long fibres of length achieving tens of meters. Note for comparison that the length of active

fibres in widely used erbium and ytterbium fibre ultrashort-pulse lasers does not exceed tens of centimetres. The use of long fibres tens of metres in length poses considerable difficulties in the development of ultrashort-pulse lasers.

We demonstrated for the first time cw generation at ~ 1160 nm in a bismuth laser in the passive mode-locked regime [9], which was initiated and maintained with the help of a semiconductor saturable-absorber mirror (SESAM) [10, 11]. The laser emitted 50-ps pulses at 1161.6 nm. Later, we investigated the dependence of the laser emission on the resonator parameters and obtained pulses of duration from 50 ps to 3.5 ns depending on the output resonator mirror [12]. The main obstacle preventing the generation of shorter laser pulses is the large positive group velocity dispersion (GVD) of a long bismuth fibre, which should be compensated by intracavity methods. There exist standard methods to control GVD, which are based on the use of prisms, diffraction gratings [13] and special fibres with the anomalous GVD [14, 15]. In this paper, we studied a bismuth-doped fibre laser using the intracavity GVD control with the help of reflection diffraction gratings, which appear to be most optimal in our case.

2. Experimental

We used an isotropic silica fibre with an aluminium–bismuth-doped core (molar concentrations of Al_2O_3 and SiO_2 were 3% and 97%, respectively, and $\text{NA} \approx 0.13$) with the fundamental-mode field diameter of 7.5 ± 0.2 μm and the second-order dispersion $\beta_2 \approx +1.43 \times 10^{-2}$ $\text{ps}^2 \text{m}^{-1}$ at 1160 nm. A preform for fibre drawing was manufactured by the SPCVD method at the laboratory of plasma-chemical technologies, FORC, RAS [16]. The atomic concentration of bismuth, determined by the X-ray structural microanalysis, was 3×10^{18} cm^{-3} . The absorption coefficient for pump radiation and the gain for radiation propagating along the fibre are small at such a low concentration of bismuth. The absorption coefficient is 1.2 dB m^{-1} at $\lambda_p = 1075$ nm and the gain at the complete saturation is smaller than 0.5 dB m^{-1} at 1160 nm. The absorption and luminescent spectra of this fibre are shown in Fig. 1.

The experimental scheme of the bismuth fibre laser is shown in Fig. 2. All the passive fibre elements of the laser cavity were fabricated of a Flexcore single-mode fibre with the fundamental mode diameter 7.3 ± 0.1 μm and $\beta_2 \approx +1.69 \times 10^{-2}$ $\text{ps}^2 \text{m}^{-1}$ at 1160 nm. The splicing loss between the active and passive fibres did not exceed 0.2 dB.

One of the mirrors of the laser Fabry–Perot resonator was a GaInNAs SESAM. This mirror was fabricated by

A.A. Krylov, P.G. Kryukov, E.M. Dianov Fiber Optics Research Center, Russian Academy of Sciences, ul. Vavilova 38, 119333 Moscow, Russia; e-mail: krylov@fo.gpi.ru;

O.G. Okhotnikov, M. Guina Optoelectronics Research Center, Tampere University of Technology, Korkeakoulunkatu 3, Tampere, 33720 Finland; RaffleKron Ltd. Ikmiestienkatu 17D 18, Tampere, 33710 Finland

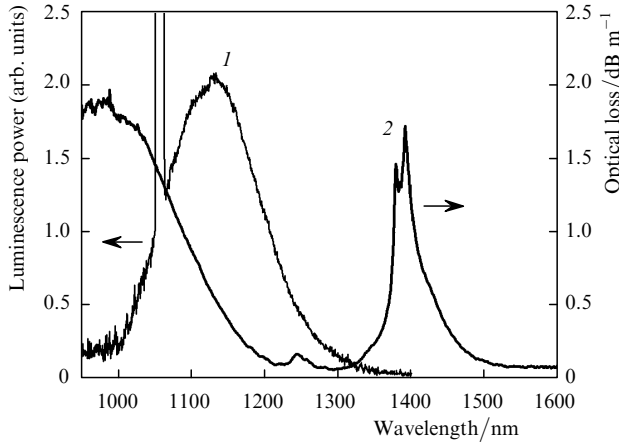


Figure 1. Luminescence [curve (1)] and absorption [curve (2)] spectra of a bismuth-doped aluminosilicate fibre. The absorption band at 1000 nm is related to bismuth, and the absorption band at 1385 nm is related to OH groups.

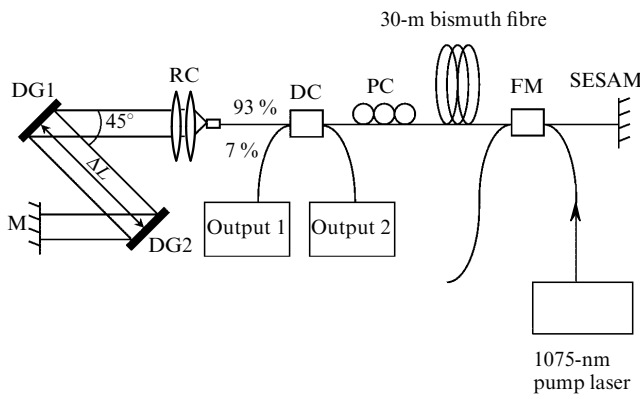


Figure 2. Scheme of the bismuth fibre laser with the intracavity GVD compensator: (FM) fibre multiplexer; (PC) polarisation controller based on a passive isotropic Flexcore fibre; (DC) 7/93 (at 1160 nm) directional coupler extracting radiation from the resonator; (DG1, DG2) reflection 600 lines mm^{-1} diffraction gratings; (M) mirror with the reflectance $\sim 100\%$ in the 1140–1250-nm band; (RC) radiation collimator based on a two-lens objective.

molecular-beam epitaxy on a GaAs substrate and optimised for operation in the spectral range from 1100 to 1200 nm [10, 11]. The SESAM operated in a nearly resonance regime, with a high contrast of the saturable radiation loss in it, because only in this case the self-starting of mode locking can occur in a laser with a positive resonator GVD [10, 11]. The end of a fibre cleaved at a right angle was either directly brought into contact with the SESAM surface or a focusing system was used between the fibre end, cleaved at an angle of 87° to its axis, and the SESAM surface, which consisted of an AR coated and corrected two-lens objective made of the TBF-10 glass.

The second mirror of the resonator was a GVD compensator based on a pair of gold-plated reflection diffraction 600 lines mm^{-1} gratings. Radiation from the output end of the fibre was collimated to a beam of diameter about 1 mm. The maximum diffraction efficiency of radiation at 1160 nm from each gating was $\sim 55\%$, being dependent on the radiation polarisation. The polarisation state was controlled with a fibre polarisation controller. The total loss in the GVD compensator, taking into account the

repeated coupling of radiation into the fibre after its optimal alignment was ~ 10.4 dB at 1160 nm. This loss and losses in other elements of the resonator were compensated by amplification in an active bismuth fibre of length 30 m. The total length of the fibre part of the resonator was 40 m, which corresponds to the total GVD approximately $+0.6$ ps^2 , whereas the anomalous GVD of the diffraction compensator was $\beta_2 \approx -1$ $\text{ps}^2 \text{m}^{-1}$. The gratings were separated by distances 37 and 55 cm, which corresponded to the anomalous GVD -0.37 and -0.55 ps^2 per pass, respectively. Our experimental conditions did not allow the use of a greater separation between the gratings required for the complete compensation of GVD in the fibre. Thus, the total GVD remained normal and was $+0.23$ and $+0.05$ ps^2 , respectively.

The laser radiation at 1160 nm was extracted with a 7% directional outcoupler, both its free ports being used for measuring laser parameters. The average output power and emission spectrum were recorded at output 1 and the pulse intensity autocorrelation function was analysed at output 2.

Pumping was performed by a home-made cw ytterbium fibre laser at 1075 nm through an insulator (with the loss and insulation of 1.5 and 25 dB, respectively, at 1075 nm) and a fibre multiplexer with the efficient combination of radiation at 1075 and 1160 nm. The pump laser was based on an ytterbium-doped fibre of length 7 m with two fibre Bragg gratings as resonator mirrors with reflectances 100% and 5% at 1075 nm. The width of the laser emission spectrum was ~ 0.05 nm and the maximum output power was 2 W. The ytterbium fibre was pumped by a 975-nm laser diode with a multimode fibre pigtail. All the passive fibre components of the pump ytterbium laser were made of a Flexcore single-mode fibre with the fundamental mode field diameter 7.0 ± 0.1 μm at 1075 nm.

The temporal parameters of laser pulses were measured with a 5-GHz Tektronix 7104 analogue oscilloscope and a germanium photodetector with the response function of duration 700 ps, as well as by an INRAD 5-14LDA autocorrelator operating in the noncollinear phase-matching regime in a lithium niobate crystal. Spectral measurements were performed by using an ANDO AQ6317B spectrum analyser with a resolution of 0.01 nm. The average radiation power was measured with a Coherent FieldMaxII power meter with a semiconductor sensor.

3. Results

The study of the laser shown schematically in Fig. 2 gave the following results. Laser pulses were generated at a repetition rate of 2.4 MHz in the passive mode-locking regime. The threshold pump power at which lasing appeared was $P_{\text{th}} = 500$ mW. Figure 3 shows the pulse intensity autocorrelation functions corresponding to different parameters of the laser resonator. The corresponding laser emission spectra are presented in Fig. 4.

The width of the autocorrelator function obtained for the distance between diffraction gratings $\Delta L = 37$ cm and, therefore, the laser pulse duration exceeded the width of the autocorrelator range (170 ps) and were virtually insensitive to variations in the radiation polarisation in the resonator. At the same time, the average output power was quite sensitive to such variations. A narrow peak at the centre of the correlation function [curve (1) in Fig. 3] demonstrates the unstable internal modulation of pulses, the peak width

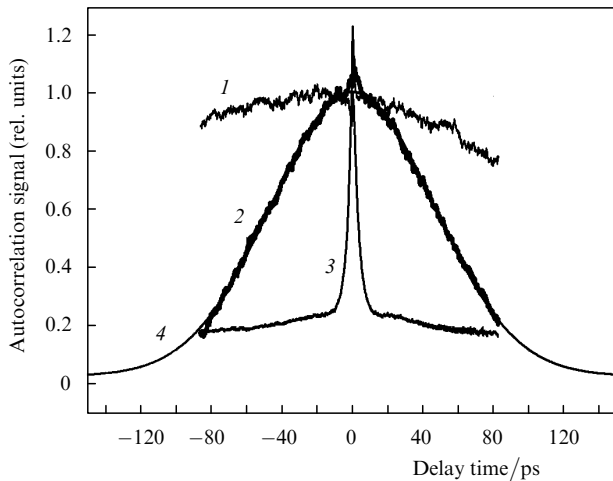


Figure 3. Intensity autocorrelation functions for pulses generated by the bismuth fibre laser for different resonator parameters: the distance between gratings $\Delta L = 37$ cm, the average output power $P_1 = 1.3$ mW, the autocorrelation function width and pulse duration $\tau_a, \tau_p \gg 100$ ps [curve (1)]; $\Delta L = 55$ cm, $P_2 = 0.15$ mW, $\tau_a = 130$ ps, $\tau_p \approx 92$ ps [curve (2)]; $\Delta L = 55$ cm, $P_3 = 0.56$ mW, $\tau_a = 7$ ps, $\tau_p \approx 5$ ps [curve (3)]; and approximation by a Gaussian [curve (4)].

corresponding to the time coherence of the pulse. The analysis of the oscilloscope signal also demonstrates pulse power fluctuations resulting in the amplitude modulation of the entire train. This is mainly related to the instability of parameters of pulses propagating in a long resonator with high losses and high gain.

As the distance between diffraction gratings was increased up to 55 cm and, therefore, the intracavity GVD decreased down to $+0.05$ ps², shorter pulses were generated [curves (2) and (3) in Fig. 3]. These autocorrelation functions differ from each other because they were obtained by varying the polarisation state and average radiation power in the resonator.

The most stable pulse train with the amplitude modulation smaller than 10 % corresponds to curve (2) in Fig. 3. In this case, the pulse duration was 92 ps for the average output power 0.15 mW (the pump power was 600 mW). Note that a decrease in the pump power resulted in a weak narrowing of the pulse intensity autocorrelation function.

Curve (3) in Fig. 3 corresponded to the minimal width (7 ps) of the autocorrelation function. When the laser passed to this operating regime, the absolute autocorrelation signal and the pulse power detected with a broadband oscilloscope increased considerably, demonstrating the increase in the radiation intensity, i.e. the narrowing of pulses. Thus, we have managed to generate pulses with the minimal duration estimated as 5 ps.

In the case of such short pulses, the role of nonlinear effects, in particular of the self-phase modulation (SPM), increases [17]. The presence of a pedestal of the autocorrelation function is probably explained by the fact that the positive frequency modulation of the pulse caused by the GVD and SPM in the fibre part of the resonator is compensated by the negative linear frequency modulation in the grating compensator only in the central part of the pulse, i.e. where it is virtually linear. This can be explained by the fact that the nonlinear frequency SPM modulation in the fibre part of the resonator greatly exceeds the linear

frequency modulation caused by the fibre GVD. In our case, the estimate of the dispersion and nonlinear lengths for 10-ps and 100-ps pulses shows that $L_D(100 \text{ ps}) \approx 500$ km, $L_D(10 \text{ ps}) \approx 5$ km, $L_{NL}(100 \text{ ps}) \approx 10$ m, and $L_{NL}(10 \text{ ps}) \approx 1$ m (the average intracavity radiation power is 7.9 mW, the nonlinear refractive index of silica is $n_2 = 3.2 \times 10^{-20}$ m² W⁻¹ [17], i.e. $L_{NL} \ll L_D$ and, therefore, SPM indeed dominates over GVD. A considerable influence of SPM is also manifested in the broadening of laser emission spectra corresponding to pulses shorter than 100 ps [curves (2) and (3) in Fig. 4]. The passage of the laser to such a regime can be caused by the influence of the nonlinear evolution of the radiation polarisation due to the induced nonlinear birefringence in the fibre (because this nonlinear nonresonance effect is of the Kerr type and is also determined by the nonlinear refractive index n_2 , the estimates of the nonlinear length for this effect made above are valid) [18–20]. Indeed, this regime was observed only when the polarisation controller was carefully adjusted and it was principally possible due to the presence of the intracavity polariser in the form of a grating GVD compensator, radiation losses in which considerably depend on the radiation polarisation, as mentioned above [21]. In fact, this laser consists of the radiation source and the fibre grating pulse compressor with non-optimal parameters, which leads to the incomplete pulse compression and the appearance of a pedestal [17].

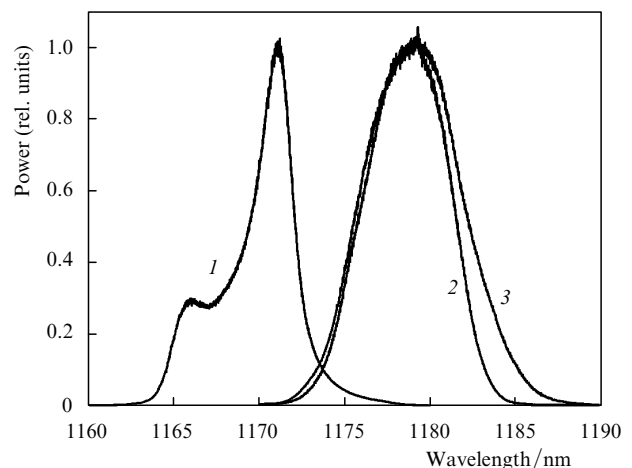


Figure 4. Emission spectra of the bismuth fibre laser for different resonator parameters: the distance between gratings $\Delta L = 37$ cm, the average output power $P_1 = 1.3$ mW, the width of the spectrum $\Delta\lambda_{FWHM} \approx 2.5$ nm [curve (1)]; $\Delta L = 55$ cm, $P_2 = 0.15$ mW, $\Delta\lambda_{FWHM} \approx 6$ nm [curve (2)]; $\Delta L = 55$ cm, $P_3 = 0.56$ mW, $\Delta\lambda_{FWHM} \approx 6.5$ nm [curve (3)].

Note also that variations in the diameter of a beam focused to the SESAM did not result in considerable changes in the operation regime of the laser, the optimal lasing conditions being achieved when the fibre end was pressed to the SESAM surface.

4. Conclusions

The bismuth-doped fibre laser has been studied with the aim of generating shorter pulses by controlling properly the intracavity GVD. Lasing has been obtained with the intracavity GVD compensator based on a pair of reflection diffraction gratings in the passive mode-locking regime,

which was initiated and maintained by using the SESAM. It has been found that upon generation of pulses shorter than 100 ps in the resonator with a partial GVD compensation, the passive mode-locking regime is very sensitive to the laser radiation polarisation, which is probably caused by the influence of the nonlinear evolution of the radiation polarisation due to the induced nonlinear birefringence when SPM dominates over GVD in the fibre part of the resonator. As far as we know, we have obtained for the first time pulses as short as 5 ps in a bismuth fibre laser at a pulse repetition rate of ~ 2.4 MHz in the wavelength range from 1160 to 1185 nm. We hope to generate in the future even shorter pulses by optimising the distance between diffraction gratings in the GVD compensator (which provides the better compensation of the frequency modulation caused by GVD and SPM in a long fibre).

Acknowledgements. The authors thank K.M. Golant and A.V. Kholodkov for the fabrication of the bismuth-doped fibre, I.A. Bufetov for recording the luminescence and absorption spectra of the bismuth fibre, A.E. Levchenko for measuring the GVD of the fibres, B.L. Davydov for the fabrication of the fibre coupler and lenses used in the study, and A.V. Tausenev for placing diffraction gratings for the GVD compensation in the resonator at our disposal. This work was supported by the Program of the Presidium of RAS ‘Femtosecond Optics and New Optical Materials’.

References

- Dianov E.M., Dvoirin V.V., Mashinsky V.M., Umnikov A.A., Yashkov M.V., Gur'yanov A.N. *Kvantovaya Elektron.*, **35**, 1083 (2005) [*Quantum Electron.*, **35**, 1083 (2005)].
- Razdobreev I., Bigot L., Pureur V., Favre A., Bouwmans G., Douay M. *Appl. Phys. Lett.*, **90**, 031103 (2007).
- Rulkov A.B., Ferin A.A., Popov S.V., Taylor J.R., Razdobreev I., Bigot L., Bouwmans G. *Opt. Express*, **15**, 5473 (2007).
- Dianov E.M., Shubin A.V., Melkumov M.A., Medvedkov O.I., Bufetov I.A. *J. Opt. Soc. Am. B*, **24**, 1749 (2007).
- Dianov E.M., Firstov S.V., Khopin V.F., Gur'yanov A.N., Bufetov I.A. *Kvantovaya Elektron.*, **38**, 615 (2008) [*Quantum Electron.*, **38**, 615 (2008)].
- Mashinsky V.M., Dvoirin V.V., Dianov E.M. *OFC/NFOEC Conf.* (San Diego, 2008) paper OThN1.
- Max C.E., Olivier S.S., Friedman H.W., An J., Avicola K., Beeman B.V., Bissinger H.D., Brase J.M., Erbert G.V., Gavel D.T., Kanz K., Liu M.C., Macintosh B., Neeb K.P., Patience J., Waltjen K.E. *Science*, **277**, 1649 (1977).
- Desurvire E. in *Proc. 31st Europ. Conf. Opt. Commun. ECOC* (Glasgow, 2005) Vol.1, p. 5.
- Krylov A.A., Dianov E.M., Dvoirin V.V., Kryukov P.G., Mashinsky V.M., Okhotnikov O.G., Guina M. *J. Opt. Soc. Am. B*, **24**, 1807 (2007).
- Okhotnikov O., Pessa M. *J. Phys.: Condens. Matter*, **16**, S3108 (2004).
- Okhotnikov O., Grudinin A., Pessa M. *New J. Phys.*, **6**, 177 (2004).
- Krylov A.A., Dvoirin V.V., Mashinsky V.M., Kryukov P.G., Okhotnikov O.G., Guina M. *Kvantovaya Elektron.*, **38**, 233 (2008) [*Quantum Electron.*, **38**, 233 (2008)].
- Diels J.-C., Rudolph W. *Ultrashort laser pulse phenomena* (NY: Academic Press, 1996).
- Lim H., Wise F.W. *Opt. Express*, **12**, 2231 (2004).
- Isomaki A., Okhotnikov O.G. *Opt. Express*, **14**, 4368 (2006).
- Bufetov I.A., Golant K.M., Firstov S.V., Kholodkov A.V., Shubin A.V., Dianov E.M. *Appl. Opt.*, **47**, 4940 (2008).
- Agrawal G.P. *Nonlinear Fiber Optics* (San Diego: Academic, 2001; Moscow: Mir, 1991).
- Maker P.D., Terhune B.W., Savage S.M. *Phys. Rev. Lett.*, **12**, 507 (1964).
- Shen Y.R. *The Principles of Nonlinear Optics* (New York: Wiley, 1984; Moscow: Nauka, 1989).
- Haus H.A., Ippen E.P., Tamura K. *IEEE J. Quantum Electron.*, **30**, 200 (1994).
- Okhotnikov O.G., Gomes L., Xiang N., Jouhti T., Grudinin A.B. *Opt. Lett.*, **28**, 1522 (2003).